Supporting Information

Shipman and Nicoll 10.1073/pnas.1217633109

SI Materials and Methods

Neuroligin (NLGN) constructs were expressed from a pCAGGS vector using a hybrid chicken β-actin/rabbit β-globin promoter with a CMV enhancer. These constructs additionally contain an internal ribosome entry site (IRES) followed by the fluorophore mCherry for visualization. Wild-type NLGN1 (mouse) and NLGN3 (human) constructs have been previously described (1). All mutations to these constructs were made using overlap-extension PCR followed by In-Fusion (Clontech) cloning. Mutations to the dimerization site were based on those originally described by Ko et al. (2) (DM1) and Dean et al. (3) (DM2 and DM3). The specific mutations were as follows: $NLGN1^{DM1}$, F458A/M459A/W463A; $NLGN1^{DM2}$, E628A/L629A; $NLGN1^{DM3}$, K622A/V623A; $NLGN3^{DM1}$, F437A/M438A/W442A; $NLGN3^{DM2}$, H606A/L607A; and $NLGN3^{DM3}$, K600A/V601A. An HA-tagged version of NLGN3 was generated by insertion of the tag between S36 and T37 in the extracellular domain. This HA-tagged NLGN3 was used only for imaging and never for electrophysiology. Molecular graphics of dimerization mutations are based on structures from Araç et al. (4) and were produced using the Chimera package from the Resource for Biocomputing, Visualization, and Informatics at the University of California, San Francisco (5). $NLGN3^{DM2}$ is also referred to simply as $NLGN3^{D\text{-}N}$ in the text and figures. pCAGGS vectors expressing GFP or mCherry alone were used for the imaging of spines in organotypic hippocampal cultures and the identification of dendrites in dissociated hippocampal cultures, respectively. The chemically inducible dimerization construct ($NLGN3^{D\text{-}N}$–iDmr) was created using $NLGN3^{D\text{-}N}$ with the addition of an FK506-binding protein (FKBP) derivative DmrB domain (Clontech) inserted at the extreme C terminus via overlap extension PCR followed by In-Fusion cloning into pCAGGS. For the induced-dimerization experiments, both $NLGN3^{D\text{-}N}$–iDmr and wild-type NLGN3 were expressed in pCAGGS following the IRES, rather than ahead of the IRES, to reduce expression due to a low level of constitutive dimerization of the chemically inducible domain at high levels of expression. The artificial dimer/chemically inducible monomer ($NLGN3^{D\text{-}N}$–revDmr) was constructed in an identical fashion with the substitution of the DmrD reverse dimerization domain (Clontech) for the DmrB domain.

1. Shipman SL, et al. (2011) Functional dependence of neuroligin on a new non-PDZ intracellular domain. *Nat Neurosci* 14(6):718–726.
2. Ko J, et al. (2009) Neuroligin-1 performs neurexin-dependent and neurexin-independent functions in synapse validation. *EMBO J* 28(20):3244–3255.
3. Dean C, et al. (2003) Neurexin mediates the assembly of presynaptic terminals. *Nat Neurosci* 6(7):708–716.
4. Araç D, et al. (2007) Structures of neuroligin-1 and the neuroligin-1/neurexin-1 beta complex reveal specific protein-protein and protein-Ca2+ interactions. *Neuron* 56(6): 992–1003.
5. Pettersen EF, et al. (2004) UCSF Chimera—a visualization system for exploratory research and analysis. *J Comput Chem* 25(13):1605–1612.

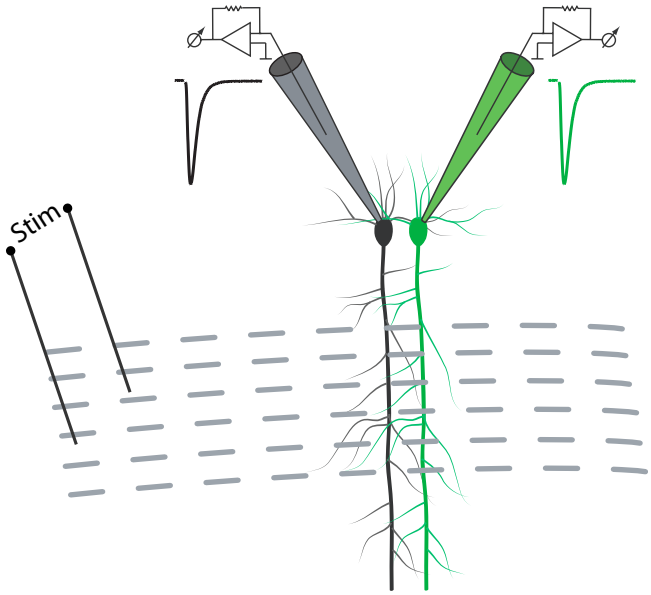

Fig. S1. Schematic diagram of the dual whole-cell recording configuration. Excitatory postsynaptic currents are simultaneously recorded in an experimental, transfected cell and neighboring control cell following evoked action potentials in the Schaffer collateral axons via a bipolar simulation electrode.

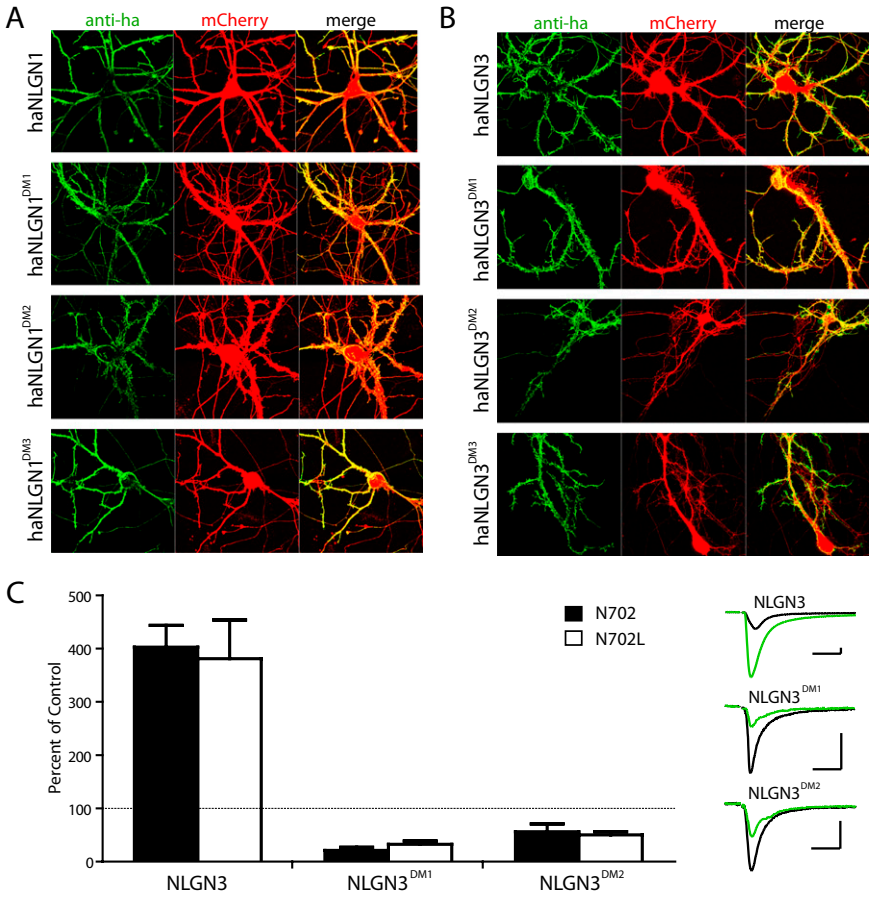

Fig. S2. Trafficking of the dimerization-null mutants. (*A*) Surface staining against an HA-tag in the extracellular domain of wild-type NLGN1, NLGN1^{DM1}, NLGN1^{DM2}, or NLGN1^{DM3} (far *Left*, in green) expressed in dissociated hippocampal neurons. Soluble mCherry marks the transfected cell (*Center*, red). Merged image is shown to the far *Right*. (*B*) As in *A*, but for HA-tagged NLGN3, NLGN3^{DM1}, NLGN3^{DM2}, or NLGN3^{DM3}. (*C*) Addition of the N702L mutant to wild-type NLGN3 ($n = 10$), NLGN3^{DM1} ($n = 10$), or NLGN3^{DM2} ($n = 10$) does not change the synaptic phenotype of postsynaptic expression in hippocampal neurons ($P > 0.05$ for wild type or either dimerization mutant N702L versus N702). Expressed as percent of control ± SEM, comparing transfected neurons in organotypic slice culture to neighboring control neurons. Sample traces (*Right*) show individual paired recordings with control AMPAR-mediated currents in black and experimental in green. (Scale bar, 20 pA/20 ms.)

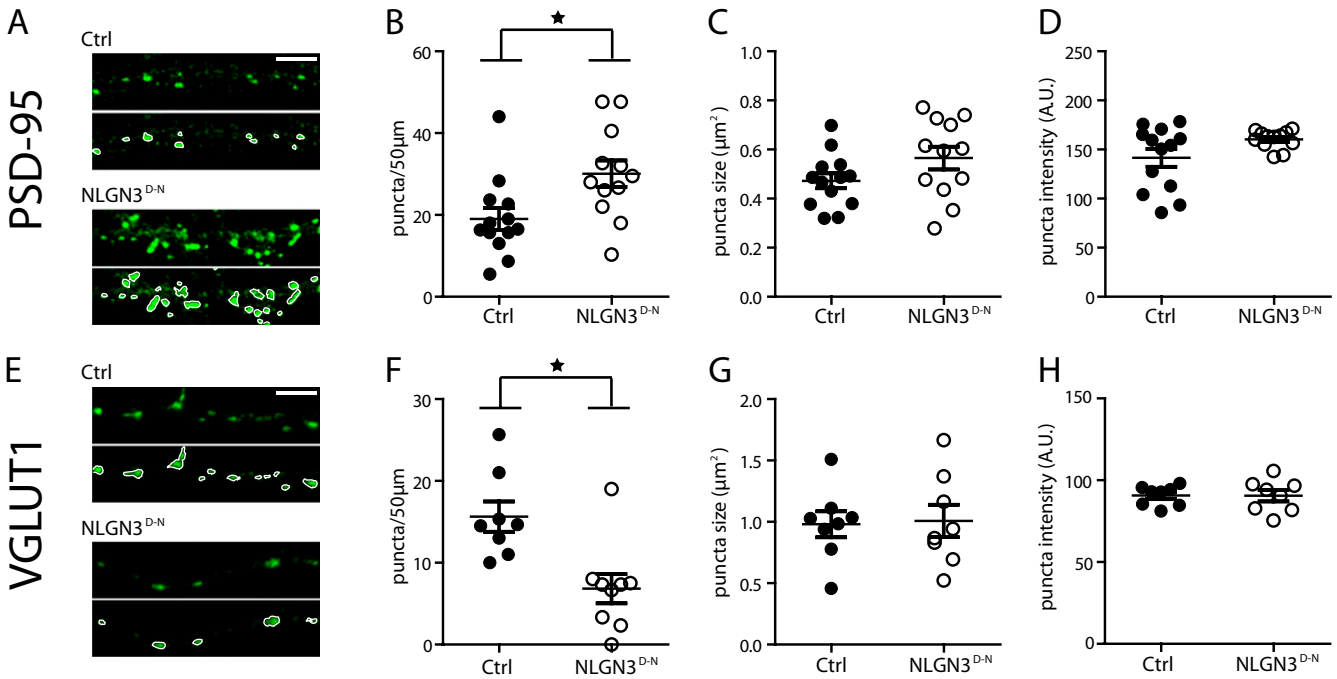

Fig. S3. Additional analysis of immunostained puncta. (*A*) Sample images of PSD-95 immunostaining for control and NLGN3$^{D\text{-}N}$ conditions. In each case, original image is shown (*Upper*) with individual puncta outlined (*Lower*). (Scale bar, 5 μm.) (*B*) PSD-95 puncta density expressed as puncta/50 μm showing an increase in density following the expression of NLGN3$^{D\text{-}N}$ [$P < 0.05$, $n = 13$ control (ctrl), 12 experimental (expt)]. (*C*) No change in PSD-95 puncta size (μm^2) following expression of NLGN3$^{D\text{-}N}$ ($P > 0.05$, $n = 13$ ctrl, 12 expt). (*D*) No change in PSD-95 puncta intensity following the expression of NLGN3$^{D\text{-}N}$ ($P > 0.05$, $n = 13$ ctrl, 12 expt). (*E*) Sample images of vesicular glutamate transporter 1 (VGLUT1) immunostaining for control and NLGN3$^{D\text{-}N}$ conditions. As in *A*, original image is shown (*Upper*) with individual puncta outlined (*Lower*) (Scale bar, 5 μm.) (*F*) Expression of NLGN3$^{D\text{-}N}$ results in a reduction of VGLUT1 puncta ($P < 0.05$, $n = 13$ ctrl, 12 expt). (*G*) No change in VGLUT1 puncta size (μm^2) following expression of NLGN3$^{D\text{-}N}$ ($P > 0.05$, $n = 13$ ctrl, 12 expt). (*H*) No change in VGLUT1 puncta intensity following the expression of NLGN3$^{D\text{-}N}$ ($P > 0.05$, $n = 13$ ctrl, 12 expt). For all scatter plots (*B–D* and *F–H*), circles represent individual cells; horizontal bars indicate mean ± SEM.